

1
2
3
4
5
6
7
8
9
10
11
12
13
14
15
16
17
18
19
20
21
22
23
24
25
26
27
28
29
30
31
32
33
34
35
36
37
38
39
40
41
42
43
44
45
46
47
48
49
50
51
52
53
54
55
56
57
58
59
60
61
62
63
64
65

Exploration of tectonic structures with GOCE in Africa and across-continent

Carla Braitenberg

Dept. of Mathematics and Geosciences, University of Trieste, Trieste, Italy

Abstract

The gravity anomaly field over the whole Earth obtained by the GOCE satellite is a revolutionary tool to reveal geologic information on a continental scale for the large areas where conventional gravity measurements have yet to be made. It is, however, necessary to isolate the near-surface geologic signal from the contributions of thickness variations in the crust and lithosphere and the isostatic compensation of surface relief. Here Africa is studied with particular emphasis on selected geological features which are expected to appear as density inhomogeneities. These include cratons and fold belts in the Precambrian basement, the overlying sedimentary basins and magmatism, as well as the continental margins. Regression analysis between gravity and topography shows coefficients that are consistently positive for the free air gravity anomaly and negative for the Bouguer gravity anomaly. The error and scatter on the regression is smallest in oceanic areas, where it is a possible tool for identifying changes in crustal type. The regression analysis allows the large gradient in the Bouguer anomaly signal across continental margins to be removed. After subtracting the predicted effect of known topography from the original Bouguer anomaly field, the residual field shows a continent-wide pattern of anomalies that could be attributed to regional geological structures. A few of these are highlighted, such as those representing Karoo magmatism, the Kibalian foldbelt, the Zimbabwe Craton, the Cameroon and Tibesti volcanic deposits, the Benue Trough and the Luangwa Rift. A reconstruction of the pre-break up position of Africa and South America (the plates forming West Gondwana) is made for the residual GOCE gravity field. The reconstruction allows the positive and negative anomalies to be compared across the continental fragments, and so helps identify common geologic units that extend across both the now-separate continents.

1 Introduction

The satellite GOCE was launched in 2009 (Floberghagen et al., 2011) with the aim to produce an improved global gravity potential Earth field. The mission requirements consisted in a global coverage, with a resolution of 100km and a precision of gravity of 1mGal at geoid level. The goals have been successfully met and the observations can be either used in terms of gradient observations along track at satellite height (250km) or

1
2
3
4 using the Earth Gravity Models (EGM) in terms of spherical harmonic expansion up to degree and order $N=250$
5 (e.g. Pail et al. 2011). The EGMs allow to calculate the gravity anomaly at any height above earth surface. The
6 advantage of using the EGM is that the complex geodetic task of averaging all GOCE gradient observations is
7 done by the specialized geodetic team. The slightly varying satellite height and the attitude changes of the
8 satellite measuring frame with respect to a Earth local north oriented fixed frame, has been fulfilled optimally
9 by the authors of the EGM. We shall use the geodetic definitions (Hofmann-Wellenhof and Moritz, 2006) for
10 the derivatives of the potential field: gravity anomaly is the analog to free air gravity anomaly used often for
11 terrestrial observations. Bouguer anomaly we call the gravity anomaly corrected for the full effect of a digital
12 terrain model discretized by prisms or tesseroids; it is the analog to the calculation of the classical complete
13 Bouguer correction, which used to be divided into the sum of the Bouguer plate and the terrain correction. We
14 call gravity effect of terrain or the terrain correction the complete effect of the digital terrain model on gravity.
15 In many parts of the world the GOCE gravity potential field is superior to terrestrial measurements, in terms of
16 resolution and precision. Locally the terrestrial field may be of higher spatial resolution, but coverage is limited
17 to a network of roads, or to specific target areas (aerogravimetry), missing the complete regional field. Further,
18 aerogravity observations are often commissioned by industry and remain undisclosed to the public. It follows
19 that GOCE makes gravity data available also in those areas where terrestrial gravity surveys have never been
20 done. In Africa important results were obtained from terrestrial gravity surveys (e.g. Hales and Gough, 1957;
21 Collignon, 1968; Louis, 1970; Slettene et al., 1973; Brown and Girdler, 1980; Browne and Fairhead, 1983), but
22 the distribution of the terrestrial data is inhomogeneous, and GOCE gives the opportunity to identify gravity
23 signals over a continent-wide scale with guaranteed equal precision and resolution. The good quality of
24 terrestrial observations is demonstrated in small differences of only a few mGal between the GOCE and
25 terrestrial fields degrading to several tens of mGal where the terrestrial data are insufficient (see e.g.
26 Braitenberg et al., 2011a,b for the Chad basin, Alvarez et al., 2012 for the Andes and Argentina and Bomfim et
27 al., 2013 for the Amazon basin in Brazil).The geologic evolution of Africa is closely linked to the geodynamic
28 evolution of the cratons constituting the continent, leading to the assemblment and break up of Pangaea,
29 Rodinia, and Gondwana. The cratons seem to be near to undeformable crustal or even lithospheric pieces
30 around which deformation in terms of rifting, sedimentation, and mountain range building occurs since
31 Proterozoic (Begg et al., 2009). These processes induce density changes in the rocks, sediments having low
32 density, rifting being often accompanied by magmatism and crustal thinning, and orogenesis by
33 metamorphism, leading to rock densification. Older belts in Africa are the greenstone belts, which formed in
34 the Archean, and include ultramafic and mafic volcanic in the lower levels of the successions, with calc-alkaline
35 and felsic volcanism in the higher levels. (Condie, 1981). Another type of Archean belts are the granulite-gneiss
36 belts consisting predominantly (80-85% surface area) of tonalite to granodiorite orthogneiss in high
37
38
39
40
41
42
43
44
45
46
47
48
49
50
51
52
53
54
55
56
57
58
59
60
61
62
63
64
65

1
2
3
4 amphibolites or granulite grade (Windley, 1984). The density changes form the link between the gravity field
5 of GOCE and the geological lineaments that can be identified. Hereby with geologic Lineament we intend a
6 linear feature of regional extent observable in a geophysical field that is believed to reflect underlying crustal
7 structure. A practical reason why the lineaments are important to trace, is in the frame of mineral exploration,
8 as mineral deposits form in specific geologic conditions and their resources depend strongly on the geodynamic
9 evolution. The Greenstone belts are favorable locations of gold mineral deposits, examples of which are the
10 Kibalian Greenstone Belt and the Greenstone Belt in Zimbabwe, which is discussed further on.

11
12
13
14
15
16 The geologically derived density variations reside in the upper crust, where the gravity signal is mixed to the
17 effect of crustal thickness variations and regional crustal density variations. The isostatic theory (Watts, 2002)
18 predicts that the topographic load be compensated at crustal level, either through lithospheric flexure,
19 producing crustal thickness variations, or through density variations that compensate the topographic load
20 (examples in orogens: Braitenberg et al. 2002; 2003; Wienecke et al. 2007). Provided the wavelengths of
21 topography are big enough (e.g. 100km), the gravity signal is proportional to the mass variations through the
22 Bouguer plate approximation. In this approximation the gravity anomaly or the Bouguer anomaly field and the
23 topographic load should have a linear relation, estimable by a regression analysis. The regression coefficients
24 represent the completeness of isostatic compensation. The deviation of the observed field from the regression
25 line is characteristic of the geologically induced density variations. The regression analysis has been successfully
26 used in the Alps (Braitenberg et al., 2013) to identify sedimentary deposits and magmatic rocks. Here we
27 calculate the regression over Africa to distinguish geologic domains through the regression result, and to
28 isolate the related gravity signal. The outcome of the study is a geologic gravity field, ready to be used for
29 hydrocarbon and mineral exploration in the aim of tracking large scale geologic lineaments (e.g. faults, rifts,
30 fold belts, sutures) and of defining the depth and geometry of the density inhomogeneities.

31 32 33 34 35 36 37 38 39 40 41 42 43 44 45 2. The GOCE gravity field in relation to topography

46
47 The gravity potential field is calculated from the spherical harmonic expansion model
48 GO_CONS_GCF_2_TIM_R4, produced by the Graz University of Technology, Institute for Theoretical and
49 Satellite Geodesy, University of Bonn, Institute of Geodesy and Geoinformation and TU München, Institute of
50 Astronomical and Physical Geodesy. It is based on 26.5 months of data, covering the period 01/11/2009 to
51 19/06/2012. It is a GOCE-only solution, where no external gravity field information is used, neither as reference
52 model, nor for constraining the solution. The calculations seek for a least squares solution using full normal
53 equations for GPS-satellite to satellite tracking and 4 components of gradiometry (V_{xx} , V_{yy} , V_{zz} , V_{xz} ; z in radial
54 direction, x along orbit, and y orthogonal to x and z) with the time-wise solution (Pail et al., 2011). The data are
55 available through ESA (<http://www.esa.int>) and at the International Centre for Global Earth Models
56
57
58
59
60
61
62
63
64
65

(ICGEM, <http://icgem.gfz-potsdam.de/ICGEM/>). The gravity anomaly with a grid spacing of 0.1° is calculated using the software of the EGM2008 synthesis and setting the parameter “isw”=01, corresponding to “spherically approximated gravity anomaly”. The height of calculation is 4000 m guaranteeing to be above topography and be able to make the topographic reduction with the data points above the topographic masses. The formal error at the full resolution of the GOCE spherical harmonic expansion (N=250) is estimated to be globally 5 mGal (Bomfim et al., 2013). Therefore every gravity variation exceeding the level of 5 mGal is a valid signal and cannot be discriminated as instrumental noise due to the downward continuation process. The GOCE derived gravity field presents an improvement with respect to existing gravity data, as has been shown in studies aimed at the evaluation of the GOCE field (Hirt et al., 2011). Complete topographic reduction was done with standard Bouguer reduction density (2670 kg/m³ over land, 1630 kg/m³ over water) in spherical approximation (Forsberg, 1984). The digital terrain model refers to the ETOPO1 (Amante and Eakins, 2009). The regression analysis is tightly connected to the isostatic compensation theory, and is fulfilled considering the equivalent topography instead of the topography, so calculations are transparent to oceanic and continental areas. The equivalent topography is defined as follows:

$$topo_equiv(x,y) = \begin{cases} topo(x,y) & \text{for } topo(x,y) \geq 0 \\ topo(x,y) * \frac{\rho_c - \rho_w}{\rho_c} & \text{for } topo(x,y) < 0 \end{cases} \quad (1)$$

Where $topo(x,y)$ is the digital elevation model, $topo_equiv(x,y)$ the equivalent topography, and ρ_c and ρ_w the crustal (2670 kg/m³) and ocean water (1040 kg/m³) densities. The topography is reduced in frequency content with a Gaussian filter of 100 km half length (e.g. Bomfim et al., 2013).

The topography is shown in Figure 1 as shaded relief map. The white outlines mark a few geological entities which have been picked out to illustrate the fact that the GOCE gravity residuals are useful in defining these geological features. This work is considering the gravity field over the entire African continent, with its geologically very diversified and complicated geology. It is impossible to consider all geological units on this scale. We therefore make a selection which shall illustrate some significant gravity signals and links to the geology. The selection has been made with the criteria of defining units rich in natural resources and that presumably generate density anomalies. The density variations are positive in case of metamorphic rocks as Greenstone belts, Fold belts, magmatic rocks, and negative in case of sedimentary sequences. The units have been digitized from the CGMW/UNESCO (1990) Geologic Map of Africa available in 6 sheets. Only the Muglad rift basin has been digitized from Dou et al. (2013). From north to south, and east to west the acronyms of Figure 1 are listed in the following. AT: Atlas Mountains. Contains dense metamorphic rocks. RS: Reguibat

1
2
3
4 shield, makes the northern part of the West African Craton. TIB: Tibesti Volcanic Mountain. ILL: Illizi Arc north
5 of the Hoggar mountains. The digitized outline embraces the Cambrian-Ordovician units of the Arc. LC: Man-Leo
6 Shield, makes the southern part of the Western African Craton. BT: Benue Trough (e.g. Fairhead, 1988). It is an
7 aborted rift basin. CV: Cameroon Volcanic Line. MB: Muglad rift basin (Sudan) with up to 13.7 km thick
8 sediments which formed in three rifting episodes between Early Cretaceous (140 Ma) to end Oligocene
9 (Mohamed et al., 2002; 2001; Dou et al., 2013). SM: Proterozoic clastic sediments (Schlüter et al. 2006).
10 PS: Archean metamorphic basement in Southern Sudan (Schlüter et al., 2006; Civetta et al. 1979). KB:
11 Kibalian belt. A Precambrian metamorphic belt including Greenstone with granitoid intrusions (e.g. Condie,
12 1981). CB: Congo basin or Cuvette Central. A large sedimentary basin. LR: Luangwa valley. A rift valley from
13 Carboniferous-Jurassic. Belongs to the Karoo system of sedimentation. ZG: Zimbabwe Greenstone belt (Condie,
14 1981; Ranganai, 2012). DB: Damara Metamorphic Belt (e.g. Gray et al., 2008). NA: Nama Group in Namibia.
15 Molasse basin type deposits (e.g. Gray et al., 2008). KV: Lebombo Mountains Karoo Volcanics and Waterberg
16 System Lava. KS: Karoo System deposits. External outline: Dwyka and Ecca series. Middle outline: Beaufort
17 series. Innermost outline marks Drakersberg stage of Karoo System, made of basalt and pyroclasts, overlying
18 the sediments. The two outer lines mark sedimentary rocks as shale, mudstone and limestones.
19
20
21
22
23
24
25
26
27
28
29
30

31 INSERT FIG 1 HERE
32
33

34 The Gravity anomaly and Bouguer fields for the African continent are shown in Figure 2.

35 The gravity anomaly shows small scale features, which are masked in the Bouguer anomaly by the great
36 contribution of the mass variations in response to the topographic load. In terms of eliminating this signal, it is
37 irrelevant whether the compensation occurs at Moho level, below it, or through densification of the crust
38 correlated to topography. In all three compensation mechanisms it is a signal that should be eliminated when
39 the focus relies on upper crustal density inhomogeneities.
40
41
42
43
44

45 INSERT FIG 2 HERE
46
47

48 3) Regression analysis and isostatic reduction 49

50 The regression analysis between gravity and topography is an alternative to the study of the local or regional
51 isostatic compensation models of the African continent. The thin plate flexure model assumes isostatic
52 compensation to be acquired through flexure of the lithosphere, which is approximated in the mathematical
53 formulation as an elastic thin plate overlying an inviscid fluid (e.f. Watts, 2002). Towards increasing
54 wavelengths, and decreasing equivalent elastic thickness, the flexural response tends towards the Airy local
55 isostatic compensation mechanism. Considering the resolution of GOCE of 80 km half-wavelength, we are
56
57
58
59
60
61

1
2
3
4 working in the wavelength band where the Airy compensation becomes a viable approximation. According to
5 the Airy hypothesis and in the approximation of the Bouguer plate, the expected relation between Bouguer
6 field and equivalent topography is linear, and the linear coefficients are:
7
8

$$BG \approx 2\pi G (r - d)(\rho_m - \rho_c) = 2\pi G \rho_c \text{ topo}_{\text{equiv}} \quad (2)$$

9
10
11
12
13
14
15 With BG the Bouguer anomaly, G the gravitational constant, r the crustal thickness, d the reference normal
16 crustal thickness, and ρ_m the upper mantle density.

17
18 In the same approximation the free air gravity anomaly should be equal to zero, because the topographic effect
19 cancels the crustal thickening effect in the Bouguer plate approximation. In reality it is found that there is a
20 small positive correlation between free air values and topography.
21
22
23

24
25 The global availability of the GOCE data presents a new opportunity to calculate the regression line between
26 Bouguer and equivalent topography over the entire African continent. We consider an average regression as
27 well as the variation of the regression for overlapping smaller windows. A homogeneous regression coefficient
28 would correspond to a uniform isostatic compensation mechanism and absence of superficial density
29 inhomogeneities. In case of a sedimentary basin with flat topography, the Bouguer field is increasingly negative
30 towards the center of the basin. Therefore the presence of the basin can be identified by the deviation of the
31 gravity signal from the average regression line. Considering local windows of analysis for the regression, an
32 area with a local density anomaly will have the effect of a scarce correlation between gravity and topography
33 and an anomalous linear coefficient. We can therefore use the linear coefficient to distinguish subsurface
34 density inhomogeneities and changes in the style of isostatic compensation. Moreover, subtracting the
35 average regression relation, the residual gravity is obtained, with enhanced signal from local density
36 variations. The two results, the residual gravity anomalies and the linear coefficients are both a means to
37 distinguish different crustal units of the African continent.
38
39

40 We run the above regression between the Bouguer field and the equivalent topography, and between the
41 gravity anomaly and the equivalent topography. Average regression coefficients are reported in Table 1.
42
43

44
45
46
47
48
49
50
51
52
53 INSERT TABLE 1 HERE
54

55
56 The regression is run twice: the second run is made on the data values that are within 1 standard deviation
57 from the regression line, in order to eliminate outliers. The regression is positive for free air anomaly and
58
59
60
61

1
2
3
4 negative for the Bouguer anomaly. The regression coefficient of free air anomaly is about one thirtieth of the
5 one of the Bouguer anomaly. The maps of the residual gravity fields are shown in Figure 3.
6
7

8
9 INSERT FIG 3 HERE

10
11 The residual fields reflect density inhomogeneities which are uncorrelated to topography and therefore to the
12 isostatic root. The regression is more effective for the Bouguer values, due to the higher regression coefficient.
13
14 The two residual fields are consistent among each other, evidencing the same density inhomogeneities. They
15 are also very similar to the free air anomaly, with the difference that the geologic signal is more focused. An
16 example is seen comparing the sequence of NNE-SSW trending gravity highs in Angola (Long. 15°, Lat. -10°),
17 which form one continuous high in Fig.2a, and several distinct gravity highs in Fig. 3a. The variation of the
18 regression coefficient is obtained by calculating the regression on sliding windows of 2° by 2°, with 75%
19 overlap. In Figure 4a the map of the regression coefficients for the Bouguer field is shown.
20
21

22
23 These coefficients are more reliable than the ones obtained for the free air field, due to their greater
24 amplitude; the standard error of the coefficients is shown in Figure 4b.
25
26

27
28
29
30 INSERT FIG 4 HERE

31
32 The scatterplots and the regression lines for each window are seen in video 1, a video which unites all
33 windows. In the video, at the top of the frame the central position of the window and the regression coefficient
34 with error are written. Each graph shows the scatterplots of Bouguer and equivalent topography and the
35 regression line. Over many windows, especially in oceanic area, the regression is linear, in some windows the
36 values can be very scattered when a local anomaly is encountered.
37
38
39
40

41
42
43 INSERT VIDEO 1 HERE

44
45 The final goal of our study is to obtain the geologic GOCE field, which is the one shown in Figure 3a,b, obtained
46 with the non-parametric method. Comparing the residual Bouguer field of Figure 3b with the original field
47 (Figure 2b), it is seen that the amplitude of the residual Bouguer has been greatly reduced, and highlights the
48 geologic signal; the amplitude of the free air anomaly (Figure 3a compared to Figure 2a) has only minor change.
49
50
51

52 53 54 4 Discussion

55
56 The regression analysis of gravity and equivalent topography is a non-parametric method to extract the
57 geologic signal from the GOCE observations. The regression has smaller scatter and greater stability in case of
58 the Bouguer field with respect to the free air anomaly. The error of the coefficient is smallest and
59
60
61

1
2
3
4 homogeneous over the ocean, in comparison to continental areas. Over the ocean the coefficient is a
5 geophysically reliable parameter, signaling changes in crustal structure. The interpretation of the coefficient is
6 an open question. A systematically more negative value covers a ribbon bordering the African continent. The
7 ribbon is from 2° to 10° wide, with largest values along the Atlantic coast southwards of the equator. The
8 ribbon seems to mark the transition to oceanic crust. Over the continent the local coefficient has greater
9 variability, due to the presence of crustal density inhomogeneities. Positive correlation coefficients for Bouguer
10 over an orogen signalize strongly increased density due to metamorphism, and is analogous to the Nettleton
11 method used to determine the density for the topographic correction of gravity measurements. The great
12 majority of the coefficient values is negative, validating the fact that the coefficient is a means to globally
13 describe the anticorrelation between Bouguer values and topography.
14
15
16
17
18
19
20
21
22

23 The residual Bouguer field is greatly reduced in amplitude, and highlights smaller scale density variations that
24 correlate to the geodynamic products as fold belts or rifting, sedimentation and magmatism. The margins of
25 the Man-Leo craton (LC) and the Reguibat shield (RS) are partly lined with a gravity signal. It is not necessarily a
26 positive signal, as would be expected for a metamorphic foldbelt, but can be also negative. Positive gravity
27 signals are found for the Tibesti (TI), the Cameroon Volcanic line (CV), the Illizi arc north of Hoggar (ILI), the
28 Damara belt (DB). The Kibalian (KB) and Zimbabwe (ZG) Greenstone belts generate a clear positive linear signal.
29 The Karoo magmatic Drakensberg deposit in Lesotho generates a well defined positive signal (KS). Same is the
30 case for the Karoo Volcanic (KV) sequence of the Lebombo Mountains along the eastern border of the South
31 African Republic. The Karoo forms an arc lining the South African coast inland (KS), continuing North-westwards
32 along the Nama sequence (NA) up to the Damara belt (DB). Clear negative signals are found for the Congo
33 basin (CB), the Benue Trough (BT) and the Luangwa Rift valley (LR). An example of the inference of geologic
34 units which are partly concealed is given in Sudan and at the Sudan-DRC (Democratic Republic of Congo)
35 border. In Sudan the Muglad rift basin (MB) generates a linear negative gravity signal of near to -30 mGal
36 amplitude. The negative signal is expected for a rift basin with a thick sequence of sediments and scarce
37 magmatism (Mohamed et al., 2001). The parallel linear gravity low which is found westwards, in DRC and CAR
38 (Central Africa Republic) along the Sudan-CAR-DRC-border has comparable amplitude and size, but must have
39 different origin, as no rift basin is known matching it. It rather correlates with the presence of Proterozoic
40 clastic sediments (PS) (Schlüter et al. 2006), which are located between the Archean basement gneisses and
41 intrusives in DRC (KB) and the Archean metamorphic basement in Southern Sudan (SM) (Schlüter et al., 2006;
42 Civetta et al. 1979). The gravity low resembles the outline of the Proterozoic sediments, though covering an
43 enlarged area and extending into the basement. If the proterozoic sediments were responsible for the gravity
44 low, they extend over a greater area than the one mapped on the general geologic map available today.
45
46
47
48
49
50
51
52
53
54

55 To illustrate the results in greater detail, Figure 5 shows the geological map (Wiles, 1971) and the residual
56 Bouguer field for Zimbabwe, together with the location of gold mines (GSC, 2013). The green units in the
57 geologic map (Figure 5a) are the outcropping Greenstones; the gold findings are associated to the
58 Greenstones, and are therefore located along or at the green patches of Figure 5. The outcropping units could
59
60
61
62
63
64
65

1
2
3
4 well be only a percentage of the complete Greenstone belt, the remainder being possibly concealed below the
5 surface. The gravity field shows an extensive regional gravity high, which correlates with the Greenstone
6 outcrops, and is generated by the entire Greenstone belt. The gold mines are found to match the gravity high
7 or its border. This demonstrates the link between the gravity high and the regional Greenstone belt, revealing
8 its dimension and orientation, also where it is concealed. If more detailed investigations of the subsurface were
9 planned, the GOCE gravity high could be used as a guideline in defining the extent and directionality of the
10 units of greater interest to mining exploration.
11
12
13
14
15

16
17 INSERT FIG 5 HERE
18
19

20 Considering the reduction of the Bouguer field, the isostatic flexure model gives similar results in terms of
21 reducing the gravity signal for crustal thickness variations, as has been done in Braitenberg (2013) for the
22 Congo basin area. The isostatic flexure model has the disadvantage that it depends on the flexure parameters
23 that must be fixed by the user. The flexure model implies crustal thickness variations being responsible of the
24 isostatic compensation, and does not consider a compensation of density variations at crustal or mantle levels.
25 This makes the regression analysis more flexible, as the latter reduces both crustal thickness and density
26 variations.
27
28
29
30
31
32
33

34 The global availability of the gravity field, allows the anomalies to be traced across continents with the aim of
35 determining a common origin, tied to the pre-break-up history. In our case of the African continent, we must
36 apply the rotations that lead to the reconstruction of western Gondwana. The reconstruction is ambiguous,
37 and depends on the specific author (e.g. Doucure' et al., 2000; Torsvik et al., 2008). Here I have chosen one
38 particular reconstruction which has made the rotation poles and the continent outlines both digitally available
39 (Torsvik et al., 2008). Details on rotation poles and continental outlines are documented in the reference
40 publication. These digital data are necessary for extracting today's gravity values and rotating them to the
41 reconstructed position. This particular reconstruction (Torsvik et al., 2009) leaves a gap between the coastlines
42 of Africa and South America, having though a tight fit along the Southern Coast of Western Africa. According to
43 the authors, the reconstruction reflects the paleomagnetic database. The discussion on the quality of the
44 reconstruction must be done elsewhere, as it is far from the topic of the present paper. Notwithstanding, the
45 major focus here is to show that the GOCE observations allow this composite field to be represented for the
46 first time at a homogeneous resolution, as it is global and has no bias from one to the other continent. The
47 reconstructed field shown in Figure 6 reflects today's crust, which has an altered density column due to the
48 processes that occurred successively to the Africa-South America separation through erosion, sedimentation
49
50
51
52
53
54
55
56
57
58
59
60
61
62
63
64
65

1
2
3
4 and magmatic emplacement. The correlation of the field between continents is masked by the events which
5 occurred after rifting. If we succeed to clean the field from the more recent events, we will be able to support
6 cross-continental geologic correlation efforts (e.g. Pankhurst et al., 2008) also at deeper crustal levels,
7 concealed to direct geologic observation. As an example we focus on the Borborema Province in Brazil which
8 connects geologically to West Central Africa (e.g. Schmus et al., 2008; De Wit et al., 2008). The Sergipano
9 domain in Brazil and the Yaounde' domain in Camerun geologically represent stacked nappes of tectono-
10 stratigraphic units which were thrust during the Brasiliano-Pan African cycle onto the San Francisco and Congo
11 cratons, respectively. Both can be traced as a gravity low. To the north, the adjacent Pernambuco-Alagoas and
12 the Adamawa-Yade' domains give a gravity high. The Tertiary volcanism of the Cameroon Volcanic Line
13 generates a linear NE-SW oriented gravity high which must be distinguished from the above signal. This
14 example shows that the new field of GOCE allows study the continuation of the geologic units through the
15 gravity field, but that the effects of the later geologic events which are uncorrelated on the two continents
16 must be reduced.
17
18
19
20
21
22
23
24
25
26

27
28 INSERT FIG 6 HERE
29
30

31 5 Conclusions

32
33 The GOCE derived gravity field is an important data set, useful in the search of natural resources as
34 hydrocarbons and minerals. The data are globally available, crossing national borders, are independent from
35 topographic changes and continent-ocean transitions. This, together with the homogeneous precision of the
36 GOCE field, guarantees global reliability of the results. Here a gravity map is offered, that reflects geological
37 boundaries and which has been freed from the disturbing signal of deep crustal origin to a great extent. A
38 selection of geologic units and lineaments are well evidenced by the gravity field. The usefulness in exploration
39 consists in identifying a signal that matches a known natural resource. The continuation of this line increases
40 the chance to encounter analogous favorable productive geologic environs. The margins of cratons have been
41 the location of crustal shortening, subduction and rifting, producing the metamorphic and magmatic rocks that
42 are essential for mineral production and the sedimentary basins that can develop to hydrocarbon reservoirs.
43 The residual gravity field that is presented here allows for the first time a cross-plate mapping of all the
44 geologic lineaments linked to density variations. The gravity field can be used in a second step for defining the
45 geometry and depth of the density units, an essential information for the geodynamic evolution. The
46 regression between Bouguer and equivalent topography is a means to characterize crustal type, as it reflects
47 the isostatic compensation mechanism. The continental margins of Africa result to change the type of
48 continent-ocean transition, with a broad transition (more than 8° width) along the southwestern margin, and a
49
50
51
52
53
54
55
56
57
58
59
60
61
62
63
64
65

1
2
3
4 width of only 3° at the western central Arica coast. This observation leads to a wider stretched crust in the
5 southern west, with respect to the northern and eastern margins.

6
7 The global availability of the field allows the geologic units to be traced across the continents, or equivalently
8 across the protocontinent as Gondwana, as is demonstrated by the composite South-America and Africa map
9 that evidences the link between several of the positive gravity anomalies identifying foldbelts that were
10 common to both continents. The cross-continent link can be done for the first time due to the great
11 improvement brought by satellite GOCE.
12
13
14
15
16
17

18 Acknowledgements

19
20 The Italian Space Agency (ASI) is thanked for supporting the GOCE-Italy project. Partially the work was
21 supported by PRIN contract 2008CR4455_003. I acknowledge the use of the EGM2008 gravity model software
22 of Pavlis et al. (2012). I thank Hans Jürgen Götze and Sabine Schmid from Christian Albrechts University Kiel for
23 inspiring discussions during the course I held in the summer semester 2013. I thank an anonymous senior
24 scientist with 40+ years of experience for his review which improved the manuscript. I thank Andre' Lambert
25 for providing the databases on mineral deposits.
26
27
28
29
30
31

32 References

- 33
34 Amante, C., Eakins, B.W., 2009. ETOPO1 1 Arc-Minute Global Relief Model: Procedures, Data Sources and
35 Analysis. NOAA Technical Memorandum NESDIS NGDC-24..
36
37 Alvarez, O., Gimenez M., Braitenberg C., Folguera, A. (2012) GOCE Satellite derived Gravity and Gravity gradient
38 corrected for topographic effect in the South Central Andes Region. *Geophysical Journal International*, 190,
39 941-959, doi: 10.1111/j.1365-246X.2012.05556.x
40
41
42 Begg, G.C., Griffin, W.L., Natapov, L.M., O'Reilly, S.Y., Grand, S.P., O'Neill, C.J., Hronsky, J.M.A., Poudjom
43 Djomani, Y., Swain, C.J., Deen, T., Bowden, P., 2009. The lithospheric architecture of Africa: Seismic
44 tomography, mantle petrology, and tectonic evolution, *Geosphere* 5, 23-50, DOI:10.1130/GES00179.1.
45
46
47 Bomfim, E., Braitenberg, C., Molina, E., 2013. Mutual Evaluation of Global Gravity Models (EGM2008 and
48 GOCE) and Terrestrial data in Amazon Basin, Brazil. *Geophys. J. Int.*, doi: 10.1093/gji/ggt283
49
50 Braitenberg, C., Ebbing, J., Götze, H.-J., 2002. Inverse modeling of elastic thickness by convolution method - The
51 Eastern Alps as a case example. *Earth Planet. Sci. Lett.* 202, 387-404.
52
53
54 Braitenberg, C., Wang, Y., Fang, J., Hsu, H.T., 2003. Spatial Variations of flexure parameters over the Tibet-
55 Quinghai Plateau. *Earth Planet. Sci. Lett.* 205. 211-224.
56
57 Braitenberg, C., 2013. A grip on geological units with GOCE. IAG Symp. 141, Springer Verlag, accepted, in
58 editorial process.
59
60
61
62
63
64
65

- 1
2
3
4 Braitenberg C., Mariani P., Pivetta T. (2011a) GOCE observations in exploration geophysics, Proceedings of the
5 4th International GOCE User Workshop, Technische Universität München (TUM), Munich, Germany 31 March
6 - 1 April 2011, 1-6.
7
8
9 Braitenberg C., Mariani P., Ebbing J., Sprlak M. (2011b). The enigmatic Chad lineament revisited with global
10 gravity and gravity gradient fields. In: Van Hinsbergen, D.J.J., Buitter, S.J.H., Torsvik, T.H., Gaina, C., and Webb, S.
11 (eds) 'The formation and evolution of Africa: a synopsis of 3.8 Ga of Earth History', Geological Society, London,
12 Special Publications, Vol. 357, 329-341.
13
14
15 Braitenberg, C., Mariani, P., De Min, A., 2013. The European Alps and nearby orogenic belts sensed by GOCE.
16 Boll. Geof. Teor. Appl., in press.
17
18
19 Brown, C. and Girdler, R.W., 1980. Interpretation of African Gravity and its implication for the breakup of the
20 continents. J. Geophys. Res., 85: 6443-6455
21
22
23 Browne, SE. and Fairhead, J.D., 1983. Gravity study of the Central African Rift System: a model of continental
24 disruption. I. The Ngaoundere and Abu Gabra rifts. In: P. Morgan and B.H. Baker (Editors), Processes of
25 Continental Rifting. Tectonophysics, 94: 187-203.
26
27 CGMW/UNESCO 1990. International Geological Map of Africa at 1:5 000 000. CGMW/UNESCO, Paris.
28
29
30 Collignon, F., 1968. Gravimétrie de reconnaissance de la République Fédérale du Cameroun. ORSTOM (Office
31 de la Recherche Scientifique et Technique d'Outre-Mer, Paris, France), 35 p.
32
33 Hales A.L. and Gough D.I. (1957) Measurements of Gravity in Southern Africa, Publisher Pretoria :
34 Staatsdrukker, 1950.
35
36
37 Condie, K.C., 1981. Archean Greenstone belts. Elsevier. Amsterdam. ISBN 0-444-41854-7.
38
39
40 Dou, L., Cheng, D., Li, Z., Zhang, Z. & Wang J. 2013. Petroleum Geology of the Fula sub-basin, Muglad basin,
41 Sudan. J. of Petrol. Geol. 36, 43 – 60.
42 Fairhead, D., 1988. Mesozoic plate tectonic reconstructions of the central South Atlantic Ocean: The role of the
43 West and Central African rift system. Tectonophysics 155, 181-191.
44
45
46 Floberghagen, R., Fehringer, M., Lamarre, D., Muzi, D., Frommknecht, B., Steiger, C., Piñeiro, J., da Costa, A.,
47 2011. Mission design, operation and exploitation of the gravity field and steady-state ocean circulation explorer
48 (GOCE) mission. Journal of Geodesy 85, 749-758.
49
50 Forsberg, R., 1984. A study of terrain reductions, density anomalies and geophysical inversion methods in
51 gravity field modelling. Ohio State University, Scientific Report N. 5, Report Number AFGL-TR-84-0174, 133 pp.
52
53
54 GSC 2013. World Mineral Deposits. Government of Canada, Natural Resources Canada, Earth Sciences Sector,
55 Geological Survey of Canada. Link: [http://gcmd.nasa.gov/records/CANADA-](http://gcmd.nasa.gov/records/CANADA-CGDI_Canada_GSC_WorldMineralDeposits.html)
56 [CGDI_Canada_GSC_WorldMineralDeposits.html](http://gcmd.nasa.gov/records/CANADA-CGDI_Canada_GSC_WorldMineralDeposits.html) (Last visited November 2013).
57
58
59 Hirt, C., Gruber, T., Featherstone, W.E. 2011. Evaluation of the first GOCE static gravity field models using
60 terrestrial gravity, vertical deflections and EGM2008 quasigeoid heights. J Geodesy 85, 723-740, DOI
61 10.1007/s00190-011-0482-y.
62
63
64
65

1
2
3
4
5 Hofmann-Wellenhof, B. and Moritz, M. 2006. Physical Geodesy, Springer Verlag, New York, ISBN 978-3-211-
6 33544-4, 403 pp.
7

8
9
10 Mohamed, A.Y., Ashcroft, W.A., & Whiteman, A.J., 2001. Structural development and crustal stretching in the
11 Muglad Basin, southern Sudan. *J. African Earth Sci.* 32, 179-191.
12

13
14 Mohamed, A.Y., Pearson, M.J., Ashcroft, W.A., & Whiteman, A.J., 2002. Petroleum maturation modelling, Abu
15 Gabra–Sharaf area, Muglad Basin, Sudan. *J. African Earth Sci.* 35, 331-344.
16

17 Pail, R., Bruinsma, S., Migliaccio, F., Förste, C., Goiginger, H., Schuh, W.-D., Höck, E., Reguzzoni, M., Brockmann,
18 J. M., Abrikosov, O., Veicherts, M., Fecher, T., Mayrhofer, R., Krasbutter, I., Sansó, F., Tscherning, C.C., 2011. First
19 GOCE gravity field models derived by three different approaches. *J. Geod.* 85/11, 819-843, doi: 10.1007/s00190-
20 011-0467-x.
21

22
23 Pankhurst, R.J., Trouw, R. A. J., Brito Neves, B. B., & De Wit, M. J. (eds) 2008. West Gondwana:
24 Pre-Cenozoic Correlations Across the South Atlantic Region. Geological Society, London, Special
25 Publications, 294.
26

27
28 Ranganai, R.T., 2012. Gravity and Aeromagnetic Studies of the Filabusi Greenstone Belt, Zimbabwe Craton:
29 Regional and Geotectonic Implications, *Int. J. of Geosci.* 3, 1048-1064, <http://dx.doi.org/10.4236/ijg.2012.35106>.
30

31 Schlüter, T., 2006. Geological Atlas of Africa. Springer Verlag, Berlin,
32

33
34 Slettene, R.L., Wilcox, L.E., Bouse, R.S., Sandvs, J.R., 1973. Bouguer Gravity Map of Africa. U.S. Defense Mapping
35 Agency, Aerospace Centre, 2nd ed.
36

37 Torsvik, T.H., Müller, R.D., Van der Voo, R., Steinberger, B., Gaina, C., 2008. Global Plate Motion Frames:
38 Toward a unified model. *Reviews Geophysics*, 46, RG3004, doi:10.1029/2007RG000227.
39

40
41 Torsvik, T.H., Rouse, S., Labails, C., Smethurst, M.A., 2009. A new scheme for the opening of the South Atlantic
42 Ocean and the dissection of an Aptian salt basin. *Geophys. J. Int.* 177, 1315–1333 doi: 10.1111/j.1365-
43 246X.2009.04137.x
44

45 Watts, A. B., 2002. Isostasy and Flexure of the lithosphere, Cambridge University Press, 2002.
46

47 Wiles, J.W., 1971. Provisional Geological Map of Rhodesia. Scale: 1000000, Publisher: The Surveyor-General,
48 Salisbury.
49

50
51 Wienecke S., Braitenberg, C., Goetze, H.-J., 2007. A new analytical solution estimating the flexural rigidity in the
52 Central Andes. *Geophys. J. Int.* 169, 789-794, doi:10.1111/j.1365-246X.2007.3396.x.
53

54 Windley, B.F., 1984. The Archean-Proterozoic boundary. *Tectonophysics*, 105, 43-53.
55
56
57
58
59
60
61
62
63
64
65

1
2
3
4
5
6
7
8
9
10
11
12
13
14
15
16
17
18
19
20
21
22
23
24
25
26
27
28
29
30
31
32
33
34
35
36
37
38
39
40
41
42
43
44
45
46
47
48
49
50
51
52
53
54
55
56
57
58
59
60
61
62
63
64
65

Figure and Table captions

Figure 1 – Topography for the African continent. The Bouguer field correlates strongly with topography, an observation that is used here to reduce the Bouguer field for the ubiquitous effects of isostatic compensation and highlight the signals generated at crustal level. Digital Elevation Model ETOPO1 (Amante and Eakins, 2009). Brown: selected geological features with acronyms (see text for details).

Figure 2 – Gravity potential fields GOCE only TIM-Release 4 (released in April 2013, method described in Pail et al., 2011) over the African continent. A) Gravity anomaly B) Bouguer anomaly. The precision and resolution of the field is homogeneous, so that each gravity variation represents a density variation in the subsurface. White: selected geological features with acronyms (see Figure 1).

Figure 3 – The residual gravity after the field correlated to topography has been removed. A) Residual of the Free Air gravity anomaly B) Residual of the Bouguer anomaly. White: selected geological features with acronyms (see Figure 1).

Figure 4 – Regression coefficient between Bouguer field and equivalent topography. A) Regression coefficient. B) Error on regression coefficient. White: selected geological features with acronyms (see Figure 1).

Figure 5 –Detail of Bouguer gravity residuals for the country of Zimbabwe (or Rhodesia). A) Geological map (Wiles, 1971), B) Bouguer gravity residual; triangles: Gold deposit (GSC, 2013). White: selected geological features with acronyms (see Figure 1).

Figure 6 – Residual gravity from regression analysis on Free Air anomaly for Western Gondwana. The correlation of anomalies across the continents highlights the mineral-bearing foldbelts which formed before the opening of the Atlantic. Details in text.

Table 1 – Average regression coefficient between equivalent topography and Free Air and Bouguer gravity fields.

Video 1 – Video showing the regression lines and scatterplots of Bouguer values against equivalent topography over the African continent on sliding windows of 2° by 2° size. At the top of the video the central coordinate of the window and the regression parameters are seen (details see text).

1
2
3
4
5
6
7
8
9
10
11
12
13
14
15
16
17
18
19
20
21
22
23
24
25
26
27
28
29
30
31
32
33
34
35
36
37
38
39
40
41
42
43
44
45
46
47
48
49
50
51
52
53
54
55
56
57
58
59
60
61
62
63
64
65

Table 1

	Regression Free Air				Regression Bouguer anomaly			
Area	b(mGal/m)	a(mGal)	errb(mGal/m)	erra(mGal)	b(mGal/m)	a(mGal)	errb(mGal/m)	erra(mGal)
EntireArea	0.0026	4.68	0.000023	0.044	-0.096	3.82	0.000023	0.043

Topography filtered

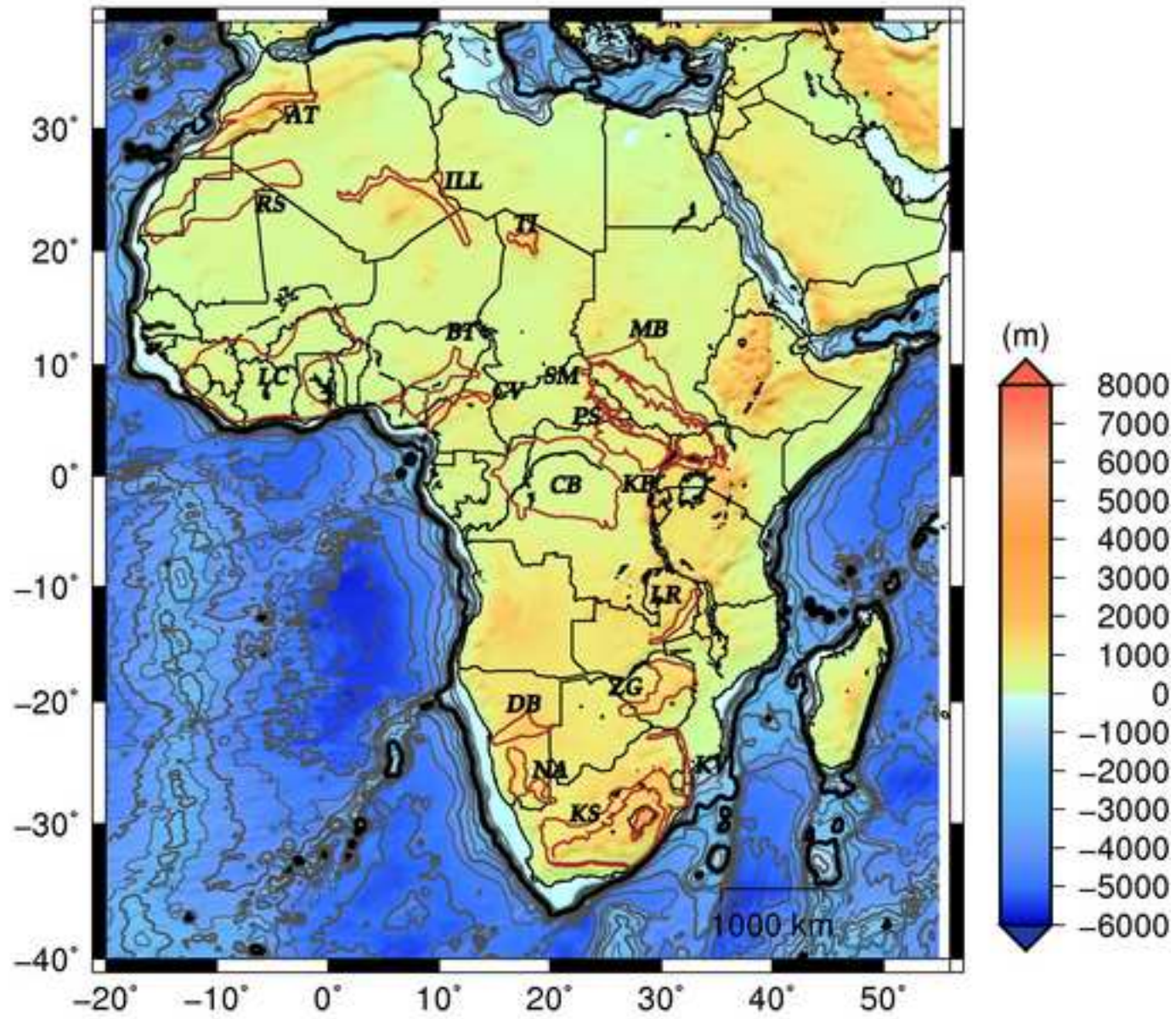


Fig.1 Etopo1

GOCE FA

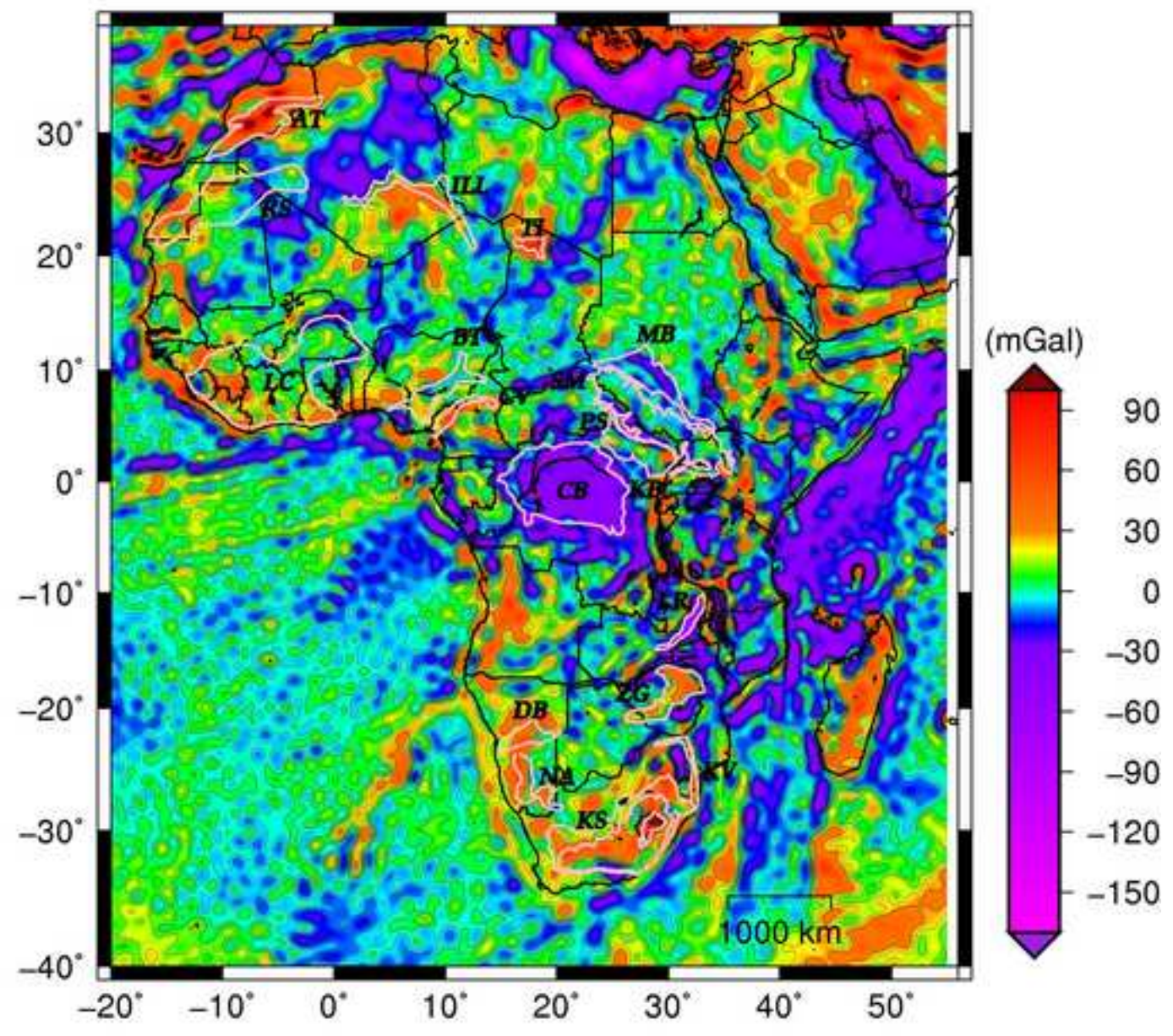


Fig.2a- GOCE FA

GOCE Bouguer

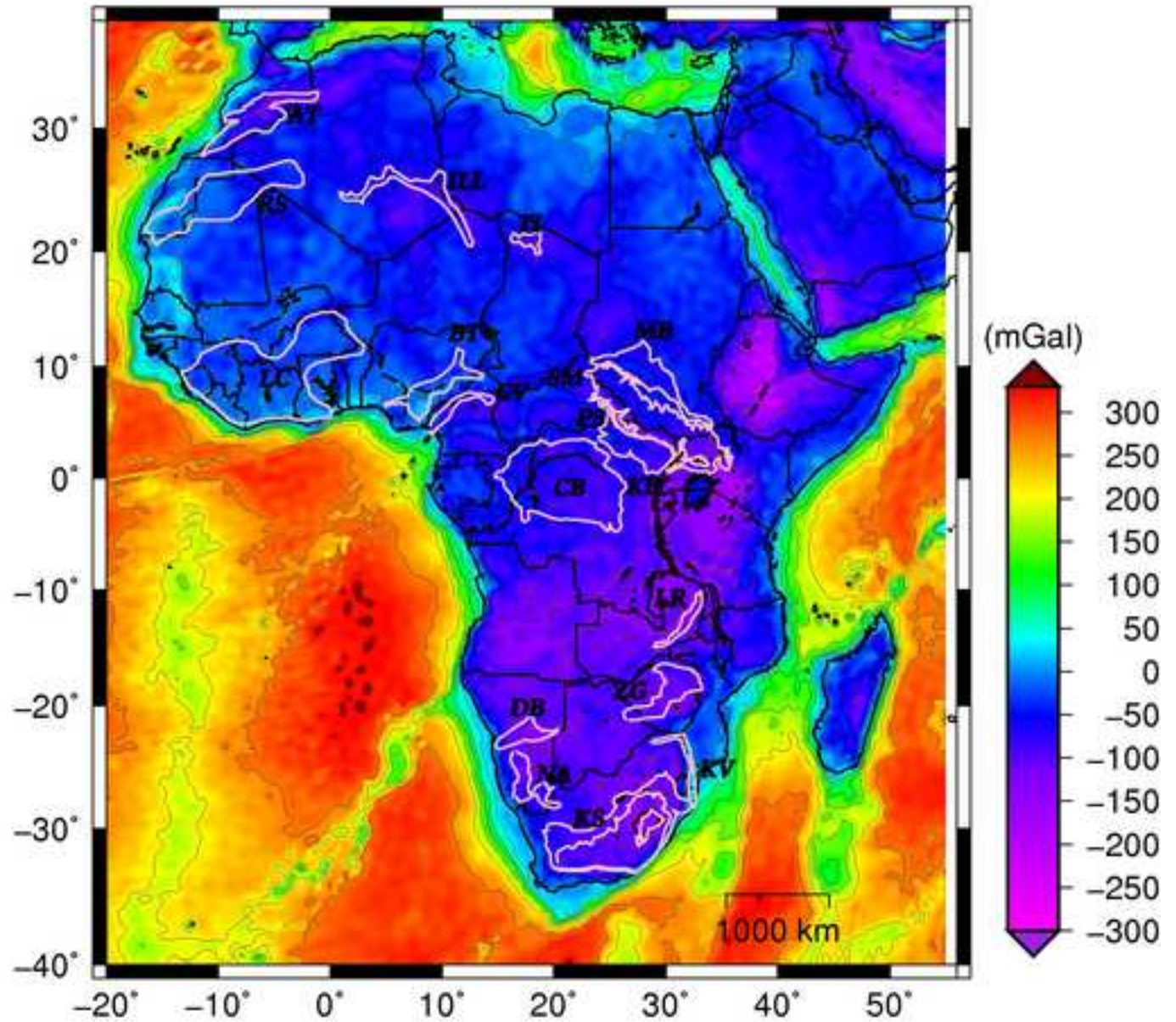


Fig. 2b- GOCE Bouguer

Residual FA GOCE TIM R4

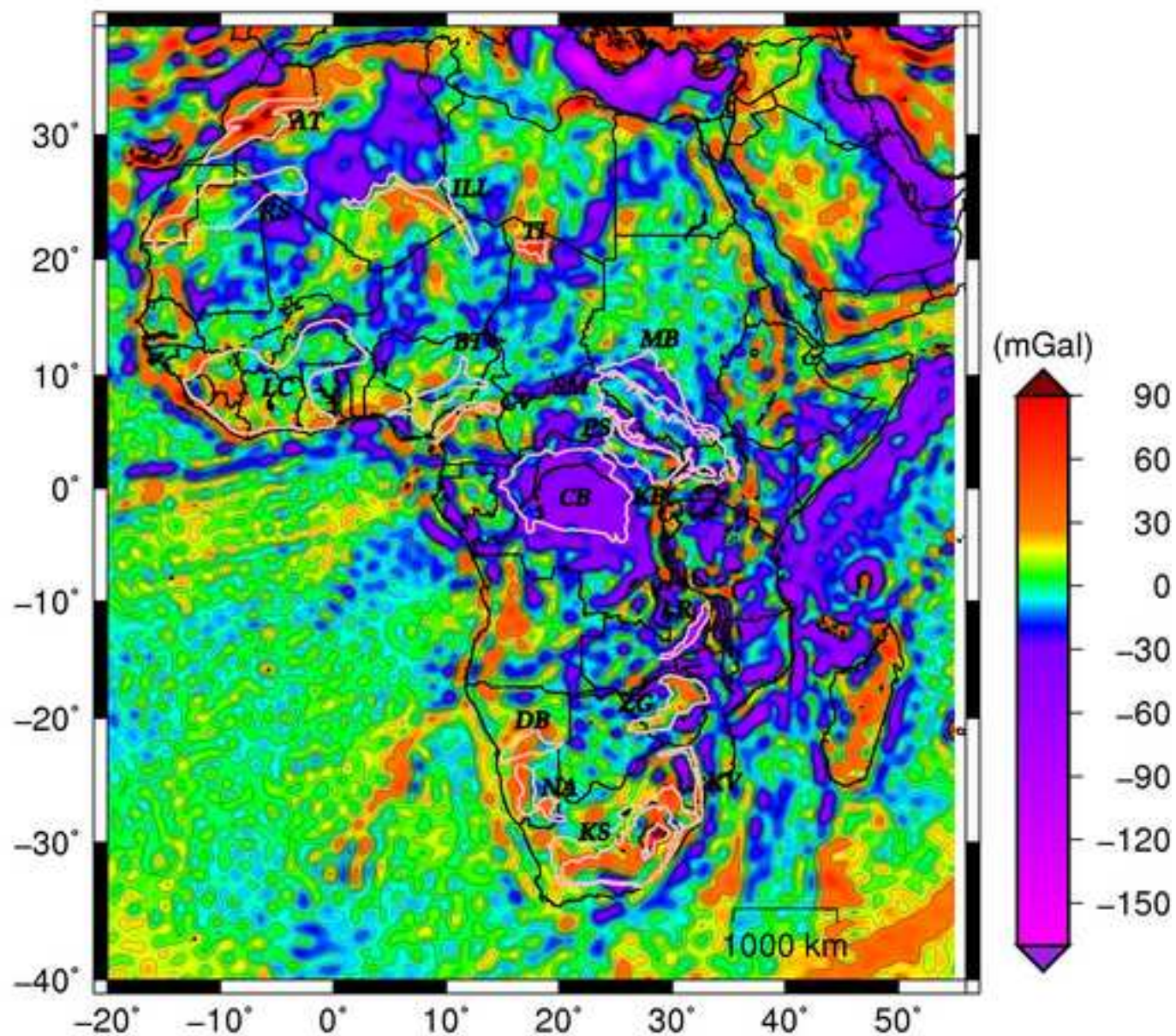


Fig. 3a Residual FA

Residual Bouguer GOCE TIM R4

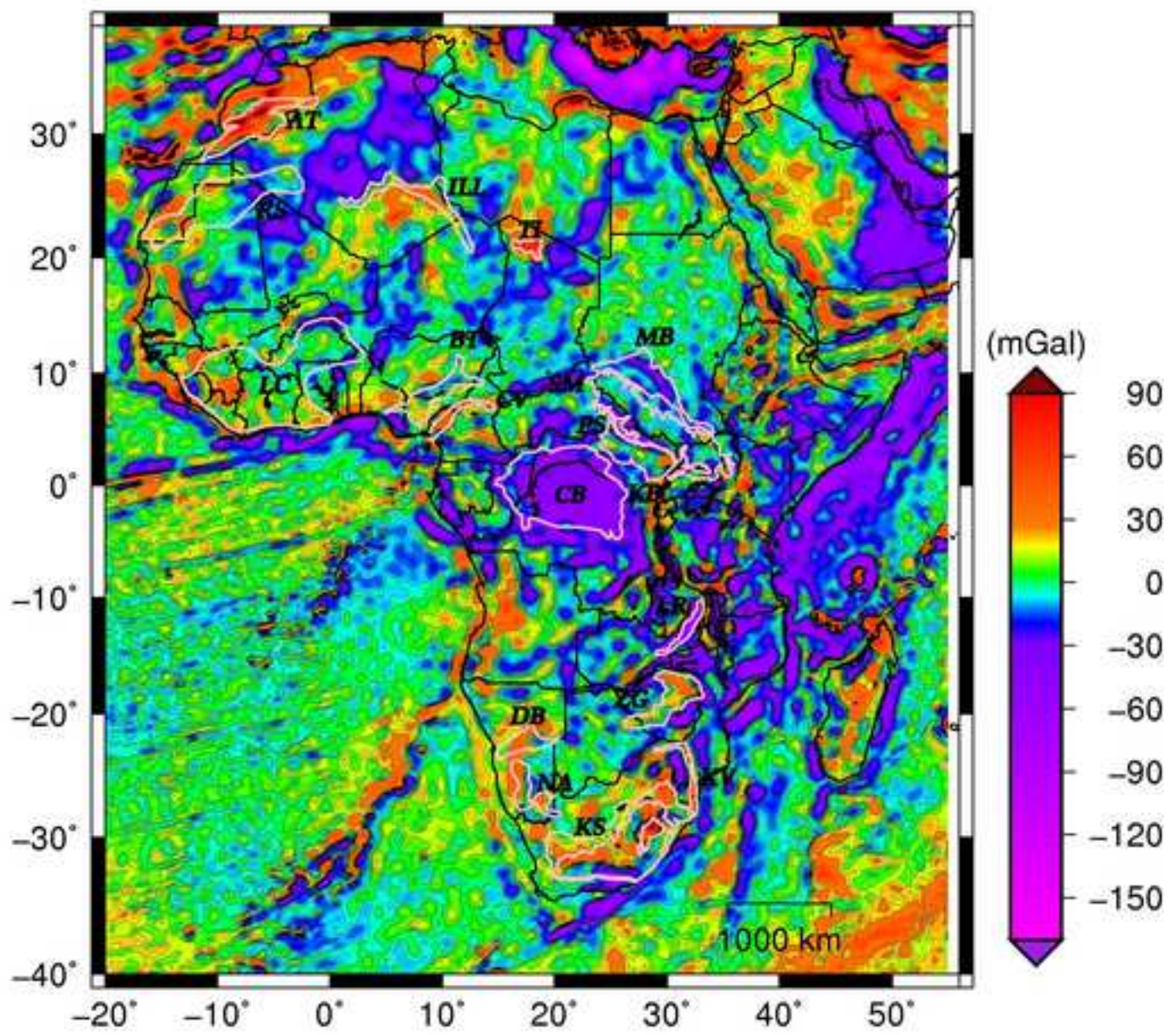


Fig. 3b Residual BG

A Regression Coefficient Bouguer

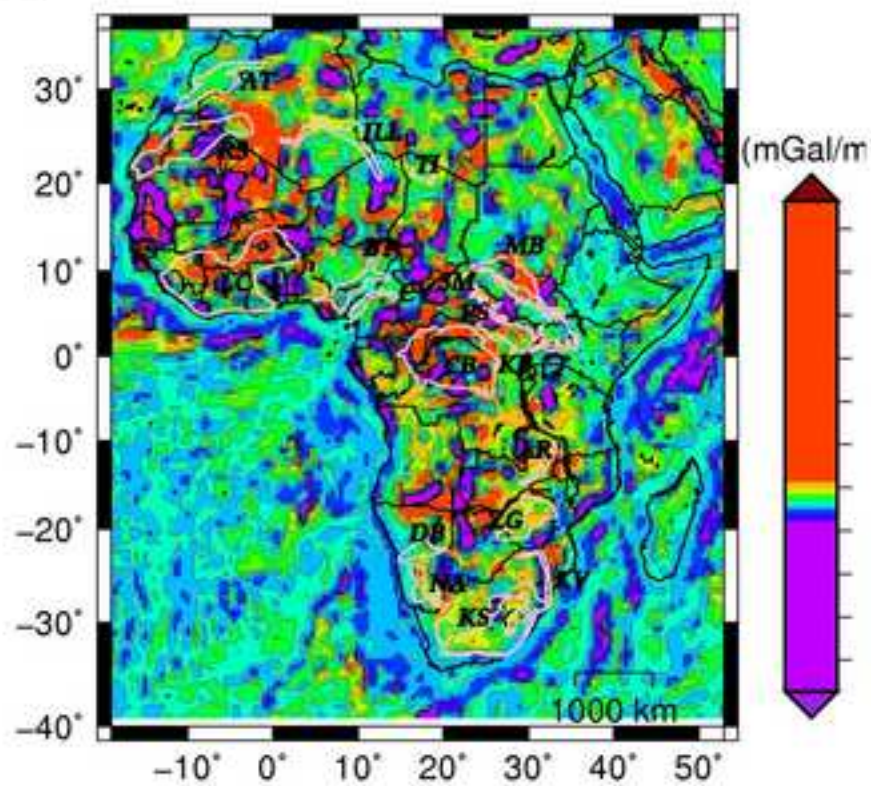


Fig.4a- Regr. Coeff.BG

B Regression Coefficient Error Bouguer

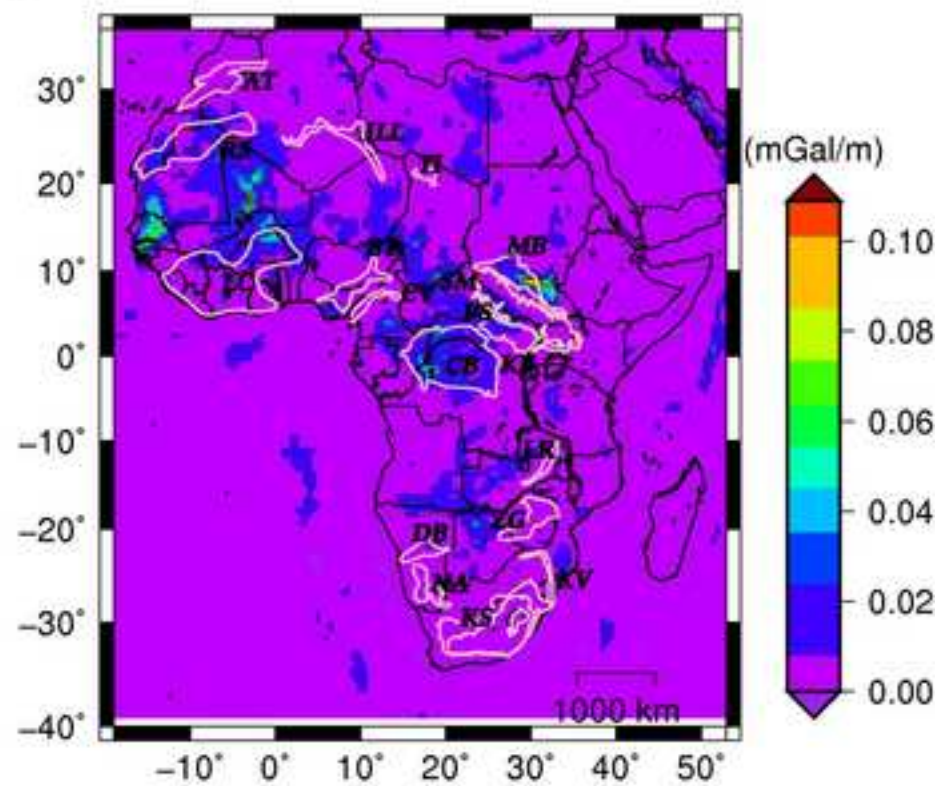


Fig.4b Regression Coefficient Error Bouguer

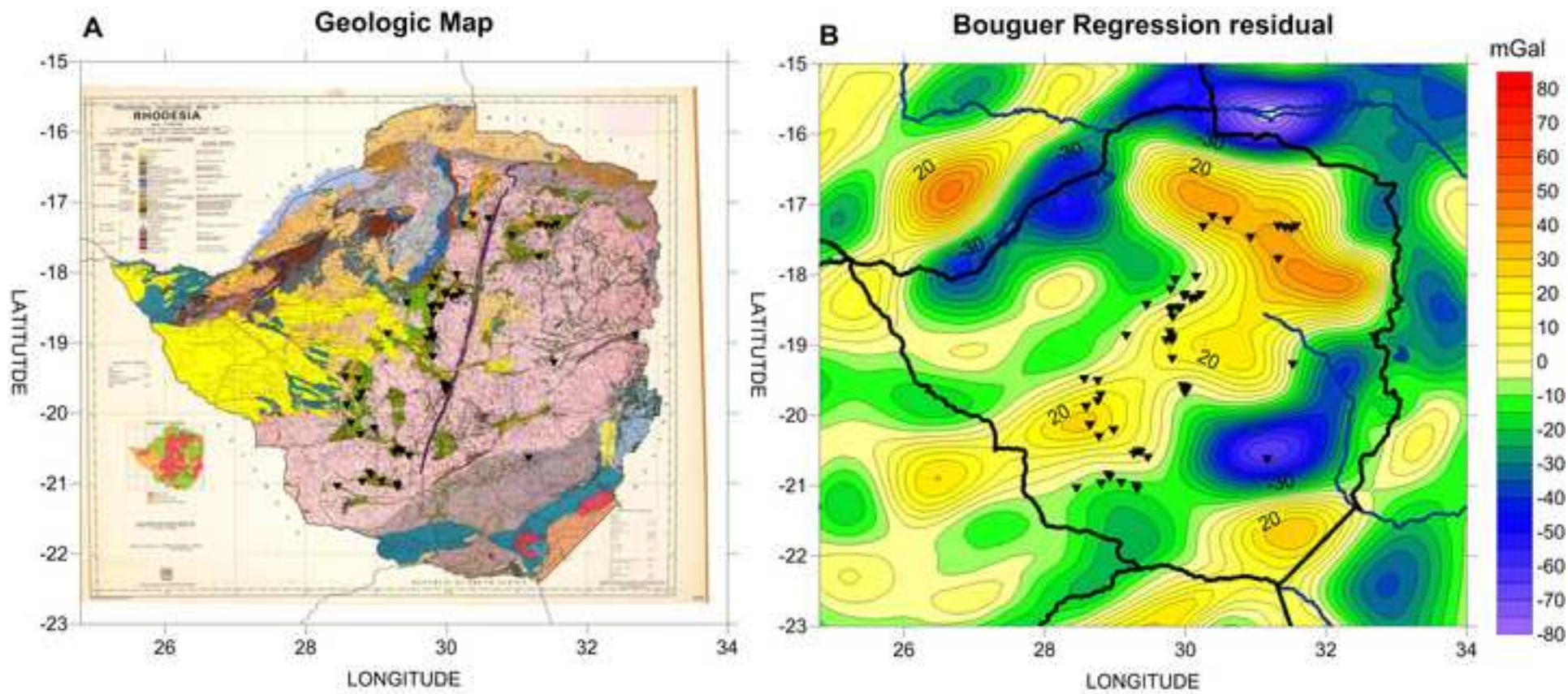
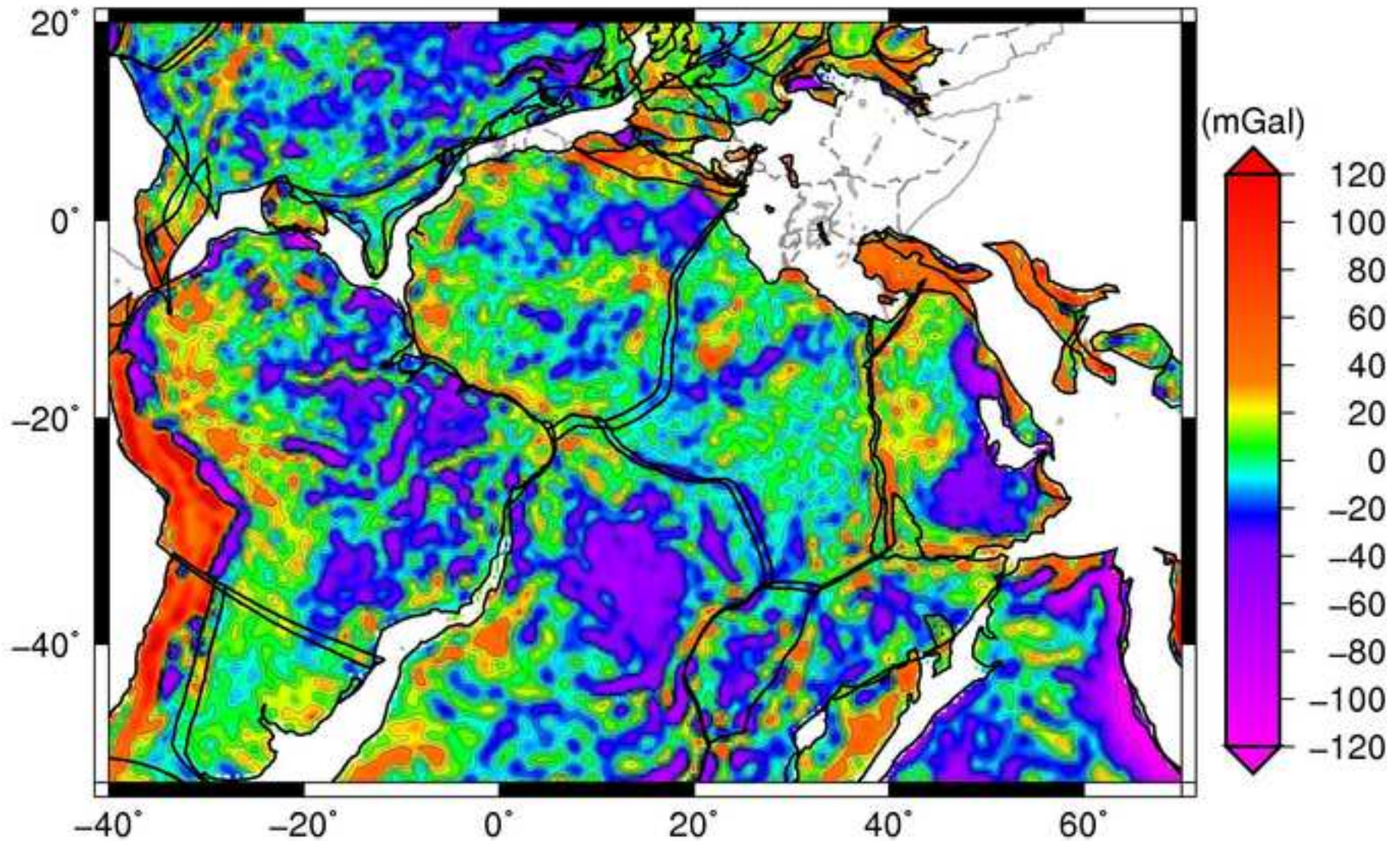


Fig6

GOCE Free Air Residual



Video

[Click here to download Video: regressions_BA_small.mp4](#)

Video Still

[Click here to download high resolution image](#)

